

RESEARCH ARTICLE

Hypomethylation of GDNF family receptor alpha 1 promotes epithelial-mesenchymal transition and predicts metastasis of colorectal cancer

Zhexu Dong¹ , Lei Dai¹ , Yong Zhang¹, Chao Fang², Gang Shi¹, Ye Chen³, Junshu Li¹, Qin Wang¹, Jiamei Fu¹, Yan Yu¹, Wenshuang Wang¹, Lin Cheng¹, Yi Liu¹, Yi Lin¹, Yuan Wang¹, Qingnan Wang¹, Huiling Wang¹, Hantao Zhang¹, Yujing Zhang¹, Xiaolan Su¹, Shuang Zhang⁴, Feng Wang^{3,5}, Meng Qiu³, Zongguang Zhou², Hongxin Deng^{1*} 

1 State Key Laboratory of Biotherapy and Cancer Center, West China Hospital, Sichuan University and Collaborative Innovation Center for Biotherapy, Chengdu, Sichuan, the People's Republic of China, **2** Department of Gastrointestinal Surgery, West China Hospital and State Key Laboratory of Biotherapy, Sichuan University, Chengdu, Sichuan, the People's Republic of China, **3** Department of Medical Oncology, Cancer Center, the State Key Laboratory of Biotherapy, West China Hospital, West China Medical School, Sichuan University, Chengdu, Sichuan, the People's Republic of China, **4** Department of biotherapy, Cancer Center, West China Hospital, Sichuan University and Collaborative Innovation Center for Biotherapy, Chengdu, Sichuan, the People's Republic of China, **5** Department of Critical Care Medicine, West China Hospital, Sichuan University, Chengdu, Sichuan, the People's Republic of China

 These authors contributed equally to this work.

* denghongx@scu.edu.cn



 OPEN ACCESS

Citation: Dong Z, Dai L, Zhang Y, Fang C, Shi G, Chen Y, et al. (2020) Hypomethylation of GDNF family receptor alpha 1 promotes epithelial-mesenchymal transition and predicts metastasis of colorectal cancer. *PLoS Genet* 16(11): e1009159. <https://doi.org/10.1371/journal.pgen.1009159>

Editor: Gregory S. Barsh, HudsonAlpha Institute for Biotechnology, UNITED STATES

Received: April 27, 2020

Accepted: September 28, 2020

Published: November 11, 2020

Copyright: © 2020 Dong et al. This is an open access article distributed under the terms of the [Creative Commons Attribution License](https://creativecommons.org/licenses/by/4.0/), which permits unrestricted use, distribution, and reproduction in any medium, provided the original author and source are credited.

Data Availability Statement: All relevant data are within the manuscript and its [Supporting information](#) files.

Funding: This study was supported by the National Natural Science Foundation of China Program grant awarded to Hongxin Deng (no. 81702349, 81772939), 1.3.5 project for Disciplines of Excellence, West China Hospital, Sichuan University (ZYGD20003) and the Fundamental Research Funds for the Central Universities awarded to Hongxin Deng (2017SCU12033) and

Abstract

Tumor metastasis is the major cause of poor prognosis and mortality in colorectal cancer (CRC). However, early diagnosis of highly metastatic CRC is currently difficult. In the present study, we screened for a novel biomarker, GDNF family receptor alpha 1 (GFRA1) based on the expression and methylation data in CRC patients from The Cancer Genome Atlas (TCGA), followed by further analysis of the correlation between the GFRA1 expression, methylation, and prognosis of patients. Our results show DNA hypomethylation-mediated upregulation of GFRA1 in invasive CRC, and it was found to be correlated with poor prognosis of CRC patients. Furthermore, *GFRA1* methylation-modified sequences were found to have potential as methylation diagnostic markers of highly metastatic CRC. The targeted demethylation of *GFRA1* by dCas9-TET1CD and gRNA promoted CRC metastasis *in vivo* and *in vitro*. Mechanistically, demethylation of *GFRA1* induces epithelial-mesenchymal transition (EMT) by promoting AKT phosphorylation and increasing c-Jun expression in CRC cells. Collectively, our findings indicate that *GFRA1* hypomethylation can promote CRC invasion via inducing EMT, and thus, *GFRA1* methylation can be used as a biomarker for the early diagnosis of highly metastasis CRC.

Post-Doctor Research Project awarded to Lei Dai (2019HXBH033). The funders had no role in study design, data collection and analysis, decision to publish, or preparation of the manuscript.

Competing interests: The authors have declared that no competing interests exist.

Author summary

Abnormal DNA methylation, one of important characteristics in tumor cells, is exploited as biomarkers for cancer diagnosis and prognosis prediction. Early diagnosis of highly metastatic CRC will be helpful for the clinical management, thus prolongs patient survival. However, it is currently difficult to make early diagnosis of highly metastatic CRC in clinical practice. Currently, we screened a novel biomarker gene, GFRA1, which associated with the invasion and poor prognosis of CRC. The targeted demethylation of GFRA1 exerted a significant promoting effect on CRC metastasis, and GFRA1 methylation-modified sequences are valuable diagnostic biomarker for CRC metastasis risk assessment. Mechanically, demethylation of GFRA1 induced epithelial-mesenchymal transition (EMT) by upregulating AKT phosphorylation and c-Jun expression in CRC cells. Our results demonstrate the promoting effect of *GFRA1* demethylation on CRC invasion and GFRA1 methylation may be a potential prognostic marker for predicting metastasis of CRC.

Introduction

Colorectal cancer (CRC) ranks third in terms of incidence and second in terms of mortality caused by cancer; more than 1.8 million new CRC cases were diagnosed and 881,000 deaths occurred from CRC in 2018 [1]. Approximately 25% of the CRC patients present metastases at the initial diagnosis stage and almost 50% of them developed metastases, contributing to the high mortality rates associated with CRC [2]. Clinically, colonoscopy is gold standard for the diagnosis of CRC [3, 4]. However, cancer metastases cannot be predicted or identified by the histopathologic or imaging examinations of colonoscopy, there is still lacking effective screening methods for CRC with high metastatic potential [5, 6]. Since invasion of the orthotopic tumors is the first step and the key point in tumor metastasis progression, thus early diagnosis of patients with highly invasive tumor cells can predict the risk of metastasis in CRC [7–9]. Although, the mechanism of invasion of CRC had been investigated previously, a specific and sensitive tumor invasion biomarker capable of predicting CRC metastasis and prognosis in the clinic is lacking [10]. Therefore, developing a novel biomarker for early diagnosis of high metastatic CRC is an effective method to improve the treatment effects and survival of CRC patients.

Substantial evidence has been accumulated suggesting that the epigenome, specifically DNA methylation has a substantial effect on the development of cancer. Therefore, changes in DNA methylation hold great promise as biomarkers for tumor risk prediction [11–13]. In previous study, hypermethylation of DNA measured in blood or stool samples could be used as a biomarker for CRC [14], indicating that DNA methylation biomarkers can be used for CRC clinical diagnosis. As compared to histopathology and imaging examinations, biomarkers can be better predictors of tumor metastasis, including that for CRC [15, 16]. Two methylation-based biomarkers that are located in the GSTpi and Sept9 gene regions are used to predict prostate and colorectal cancers and have been approved by the US FDA, showing that methylated biomarkers have great potential for clinical diagnosis and prediction of cancers [17, 18]. In addition, hypermethylated NEUROG1, RASSF1A, RASSF2A, SDC2, SEPT9, TAC1, and THBD genes were detected in early stage CRC, hypermethylation of ALX4, FBN2, HLTF, P16, TMEFF1, and VIM genes was associated with poor prognosis, and hypermethylated P16 and TFPI2 genes were related to recurrence of CRC [14]. However, few studies on DNA methylation biomarkers associated with CRC invasion or as predictors of metastasis have been reported.

Glial cell derived neurotrophic factor receptor alpha 1 (GFRA1), a member of the GDNF ligand family, plays important roles in nervous system development, spermatogenesis and tumor progression [19]. Previous studies found GFRA1 regulates the proliferation and differentiation of nerve cells [20, 21] and spermatogenic stem cells via binding GDNF ligand [22–24]. Meanwhile, GFRA1 gene can be methylated during spermatogenesis [25]. In addition, GFRA1 can promote the proliferation and migration in pancreatic cancer and breast cancer [26, 27], and induce chemotherapy resistance in osteosarcoma [28]. However, the function and methylation level of GFRA1 in CRC is still not clear.

In order to discover a CRC invasion related DNA methylation biomarker, we used TCGA database data in combination with CRC patient prognostic data to screen for the potential biomarker, which could be associated with CRC tumor invasion and prognosis. GFRA1, a cancer-promoting gene in pancreatic and breast cancers [26, 27], was selected for further analysis. Furthermore, we used dCas9-mediated DNA methylation editing to target demethylation of the GFRA1 gene and investigate the potential function and mechanism of GFRA1 in regulating metastasis in CRC. Our results suggest that *GFRA1* methylation can be used as a biomarker for the early diagnosis of metastasis-risk CRC.

Results

Hypomethylation mediated upregulation of GFRA1 correlated with invasion and poor prognosis of CRC

To screen for potential genes that were regulated by methylation in CRC, we analyzed the RNA-seq data and methylation data in 38 normal tissues and 309 Colon adenocarcinoma (COAD) tumor tissues from The Cancer Genome Atlas (TCGA), in which 65 hypermethylated genes with significant down-regulation of RNA levels were found (S1A and S1B Fig, Fig 1A). After that, we compared the methylation and mRNA expression level of candidate genes between invasive and non-invasive CRC tumors. Among these genes, GFRA1 was screened for its significant hypomethylation and high expression in invasive CRC compared to non-invasive colon cancer (Fig 1B and 1C). Furthermore, the clinical relevance of GFRA1 in CRC was determined based on the TCGA database. The results suggested that GFRA1 methylation levels were significantly reduced and the mRNA levels were significantly elevated in patients with lymphatic invasion and vascular invasion (Fig 1D and 1E). Next, correlation analysis from TCGA and HXCRC cohort showed that the methylation levels of GFRA1 were slight negatively correlated with the gene expression (Fig 1F and 1G). The treatment of CRC cell lines with anti-methylation drug DAC could significantly increase the expression of GFRA1 (S1C–S1E Fig), this indicates that GFRA1 expression could be upregulated by GFRA1 demethylation. Then, the GFRA1 mRNA expression was determined in a HXCRC cohort containing 90 malignant tissues of CRC patients. The analysis indicated that the high expression of GFRA1 is consistently correlated with shorter overall survival and disease-free survival (Fig 1H). Furthermore, we also got similar results on the HXCRC cohort tissue microarrays (TMA) containing 251 malignant tissues of CRC patients based on the GFRA1 protein expression (Fig 1I, S1F Fig). Taken together, these results suggested that hypomethylation-mediated GFRA1 upregulation associated with metastasis and poor prognosis of CRC patients.

GFRA1 hypomethylation associates with tumor invasion and poor prognosis in CRC

To further explore the relationship between *GFRA1* methylation and tumor invasion, we performed a full-length methylation modification analysis of *GFRA1* using 450K methylation

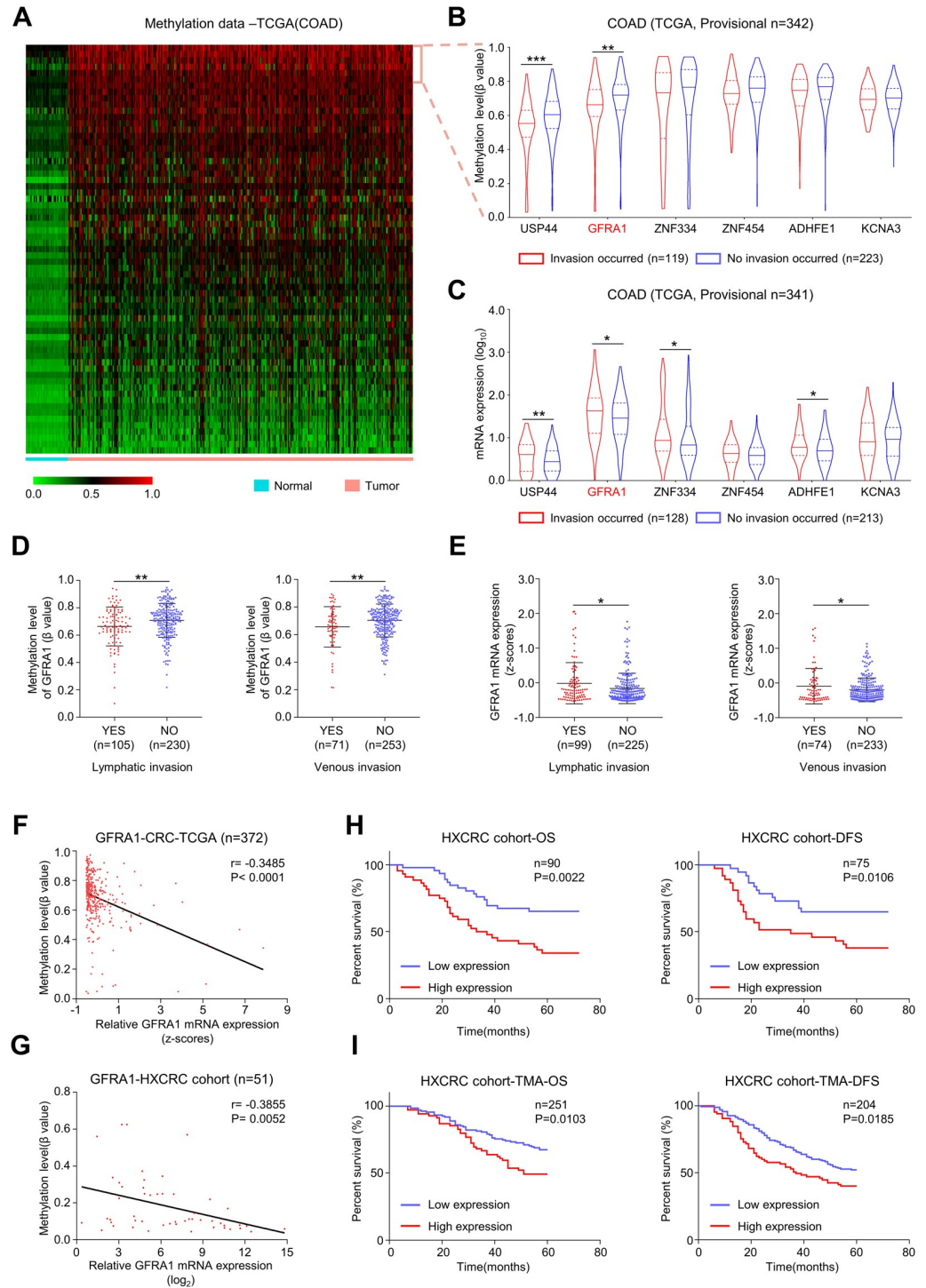


Fig 1. Hypomethylation mediated upregulation of GFRA1 in colorectal cancer is associated with tumor invasion and poor prognosis. **A** Heat map showing associated with the methylation profile of 65 genes in normal and tumor tissues from S1A Fig, β value indicating the DNA methylation levels are represented by the color of the heat map (Red means high methylation, green means low methylation). **B** Violin plot of differentially methylated genes in CRC tumors with or without invasion based on TCGA (** $p < 0.01$, *** $p < 0.001$; student t-test). **C** Violin plot of differentially expression level of methylated genes in CRC tumors with or without invasion based on TCGA (* $p < 0.05$, ** $p < 0.01$; student t-test). **D** Comparison the GFRA1 gene methylation in tumors with or without lymphatic invasion and venous invasion from TCGA (** $p < 0.01$; student t-test). **E** Comparison the GFRA1 mRNA expression (z-scores relative to diploid samples) in tumors with or without lymphatic invasion and venous invasion from TCGA (* $p < 0.05$; student t-test). **F** Correlation analysis between GFRA1 gene expression (z-scores relative to diploid samples) and methylation levels

from TCGA (Pearson's correlation test). **G** Correlation analysis between GFRA1 gene expression and methylation levels from HXCRC cohort patient samples (Pearson's correlation test). **H** Overall and disease-free survival of patients from HXCRC cohort GFRA1 RNA expression data (log-rank (Mantel-Cox) test). Data are mean \pm SD. **I** Overall and disease-free survival of patients from HXCRC cohort GFRA1 protein expression data (IHC staining in TMA, log-rank (Mantel-Cox) test). Data are mean \pm SD.

<https://doi.org/10.1371/journal.pgen.1009159.g001>

chip data derived from TCGA. As compared to the non-invasive tumor tissues, the significantly hypomethylated region in the invasive tumor was mainly located in the CpG island of the transcription start site (TSS) (Fig 2A). Combining clinical invasion phenotype and *GFRA1* expression correlation analysis, we found 10 eligible probe sequences (Fig 2B and S1 Table). Among them, three sequences are located upstream of the TSS, and seven sequences are located downstream of the TSS (Fig 2A). In further analysis, the three probe sequences upstream of TSS were found to be negatively correlated with the gene expression (Fig 2C–2E). The methylation level of this sequence was also significantly reduced in stage 3–4 colon cancer tissues, and in tumor tissues with lymphatic invasion and vascular invasion (Fig 2C–2E). The other seven probe sequences downstream of TSS were found to have similar results (S2 Fig). To further evaluate the performance of *GFRA1* methylation in predicting CRC invasion, ROC curves were initially calculated using probe sequence data with significantly reduced methylation levels ($P < 0.001$) in lymphatic invasive tumors. As shown in S3 Fig, the AUC values of the eight probe sequences ranged from 0.6 to 0.7, indicating that *GFRA1*-low methylation can be used as a methylation biomarker for tumor invasion. After that, we used 92 clinical patient samples (75 tumor tissues and 17 paracancerous tissues) to determine the degree of methylation upstream of *GFRA1* TSS by time-of-flight mass spectrometry. The methylation sites around the cg25617725 probe sequence have higher methylation modification in colon cancer patients (Fig 2F), but hypomethylated patients with shorter overall survival and disease-free survival (Fig 2G). In summary, *GFRA1* epigenetic modification sequences in TSS associated with tumor invasion and poor prognosis.

dCas9-TET1CD mediated *GFRA1* specific demethylation

To test whether demethylation of the hypermethylated TSS can reactivate *GFRA1*, we constructed gRNA-mediated *GFRA1*-targeted methylation editing plasmid (Fig 3A). This plasmid recruits dCas9-TET1CD to the TSS of *GFRA1* via gRNA [29], thus specifically demethylating the TSS region of *GFRA1*. We found that most of the *GFRA1* gene in CRC cell lines has high methylation modifications in the CCLE database (S4A Fig). Therefore, HCT116 and SW480 cells, which show hypermethylation of *GFRA1* by BSP sequencing (S4B Fig), were used for targeted *GFRA1* demethylation. We designed eight gRNAs and selected the two best gRNAs (gGFRA1-5 and gGFRA1-6) based on the *GFRA1* protein expression in western blotting (Fig 3B, S2 Table). Furthermore, we subsequently proved that dCas9-TET1CD-gGFRA1-5 and dCas9-TET1CD-gGFRA1-6 significantly removed the *GFRA1* gene methylation and upregulated the *GFRA1* mRNA expression in HCT116 and SW480 cells (Fig 3C and 3D). Since our DNA targeting methylation editing system is mediated through the use of gRNA, it was required to determine whether gene-targeted demethylation was off target. By using the gRNA off-target sequence prediction website (<https://crispr.bme.gatech.edu/>), we identified the 10 most likely off-target sites for gGFRA1-5 and gGFRA1-6 (S3 and S4 Tables). Among them, the gGFRA1-5 off-target site corresponds to 9 genes (CCDC172, LRMDA, ZNF730, THNSL2, GABRG2, CBLB, FAM22A, EFNB2, and SLC14A2), and the gGFRA1-6 off-target site corresponds to 3 genes (CCDC172, TMEM18, and NFASC). We further used qRT-PCR to detect gene expression of the gRNA off-target sites after transfection of dCas9-TET1CD-gGFRA1-5

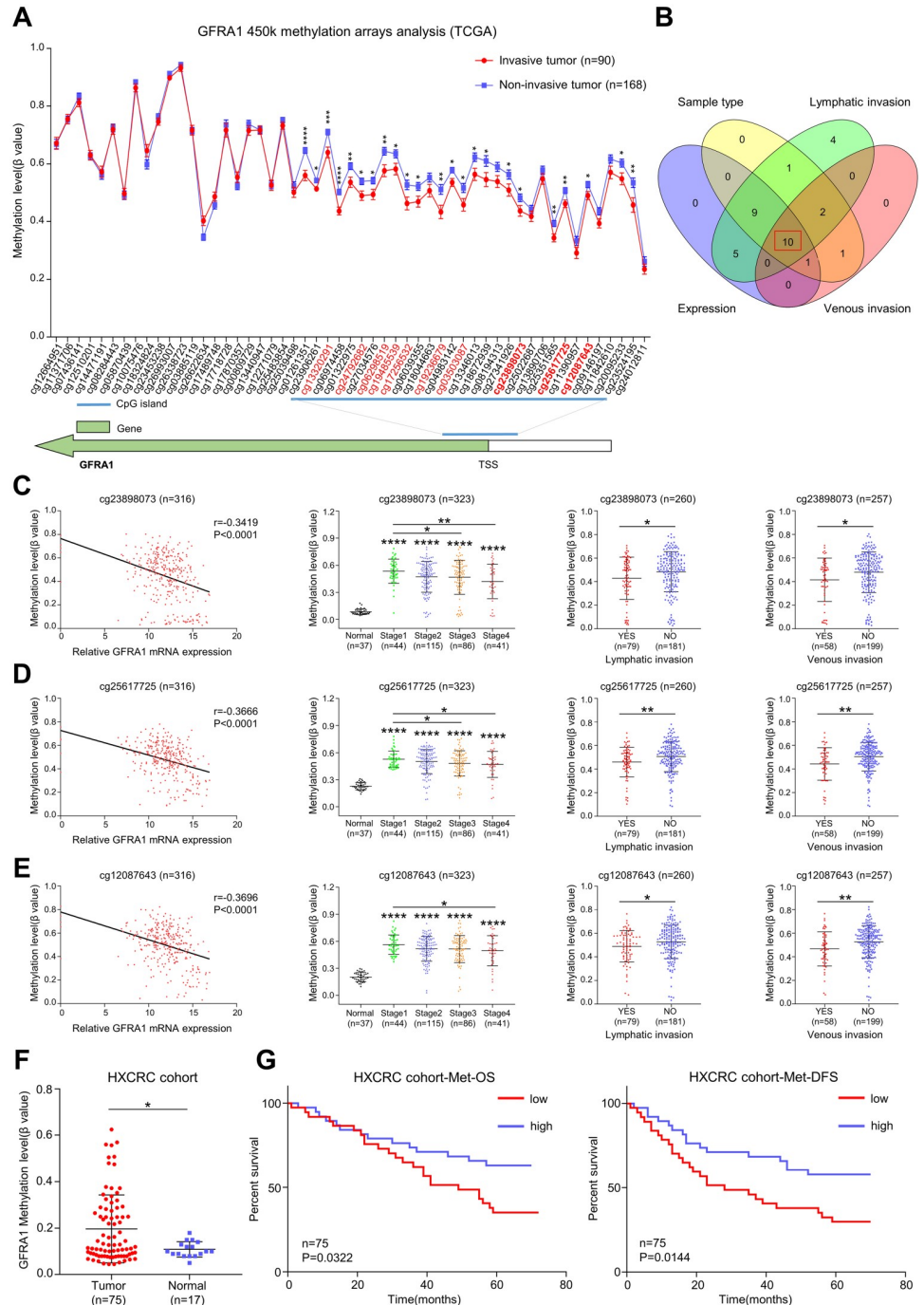


Fig 2. Analysis of full-length methylation modification of GFRA1 gene in CRC based on 450K methylation microarray. **A** Full-length 450K methylation array data analysis of GFRA1 gene in invasive CRC tumors compared to non-invasive CRC tumors (* $p < 0.05$, ** $p < 0.01$, *** $p < 0.001$, **** $p < 0.0001$; student t-test, Data are mean \pm SEM). **B** Venn diagram used to demonstrate a common list of 10 methylated sequences. Including the correlation between the probe sequences DNA methylation level and gene expression ($r < -0.3$; Pearson's correlation test, Expression), the methylation modification of probe sequences in CRC ($p < 0.05$; student t-test, Sample type), significant reduction of DNA methylation level in lymphatic invasive CRC ($p < 0.05$; student t-test, Lymphatic invasion) and vascular invasive CRC ($p < 0.05$; student t-test, Venous invasion). marked in red in (A). **C-E** Detailed description of three methylation sequences upstream of GFRA1 gene TSS from (B), including correlation between gene expression and DNA methylation (Pearson's correlation test), variety in DNA methylation levels at different tumor stages (* $p < 0.05$, ** $p < 0.01$, *** $p < 0.0001$; student t-test) and differences in methylation levels between invasive and non-invasive

tumors (* $p < 0.05$, ** $p < 0.01$; student t-test). F Comparison of the methylation levels of *GFRA1* TSS upstream in CRC tumor tissues and normal tissues from HXCRC cohort (* $p < 0.05$; student t-test). G Overall and disease-free survival of patients from HXCRC cohort methylation data in (F) (log-rank (Mantel-Cox) test). Data are mean \pm SD.

<https://doi.org/10.1371/journal.pgen.1009159.g002>

and dcas9-TET1CD-gGFRA1-6 in HCT116 and SW480 cells. It was found that *GFRA1*-targeted methylation editing plasmid did not cause significant changes in the off-target gene expression (Fig 3E and 3F and S4C and S4D Fig). Collectively, dcas9-TET1CD-gGFRA1-5 and dcas9-TET1CD-gGFRA1-6 could induce targeted and specific demethylation of *GFRA1* in CRC.

Targeted demethylation of *GFRA1* promotes CRC metastasis

To test whether *GFRA1* hypomethylation will promotes CRC metastasis, HCT116 cells after transfection with dcas9-TET1CD-gGFRA1-5 or dcas9-TET1CD-gGFRA1-6 were injected into the tail vein of BALB/c nude mice. One month after HCT116 cell injection, the organ metastases in nude mice were determined. As shown in Fig 4A and 4B, more lung metastasis nodules were observed in the groups with *GFRA1* hypomethylation, as compared to the control group. Next, we evaluated the ability of *GFRA1* targeted demethylation on the proliferative capacity of HCT116 and SW480 cells using CCK8 proliferation assay and colony formation assay *in vitro*. The results indicated that the proliferative capacity of HCT116 cells and SW480 cells was significantly enhanced after removal of *GFRA1* methylation (Fig 4C). Similarly, the colony formation assay suggested that the targeted demethylation of *GFRA1* also significantly increased the number of clones produced by CRC cells after two weeks (Fig 4D). Moreover, the effect of *GFRA1* hypomethylation on the motility and invasion capability of CRC cells *in vitro* was detected in Transwell assay. After incubating for 48 h, the *GFRA1*-targeted demethylation significantly increased the migration and invasion of HCT116 and SW480 cells (Fig 4E and 4F). These results suggest that *GFRA1* hypomethylation may serve as a tumor promoting factor to induce the metastasis of CRC, as shown in previous clinical data analysis results.

Targeted demethylation of *GFRA1* gene induces epithelial to mesenchymal transition in CRC cells

To further explore the mechanism of *GFRA1* targeted demethylation in promoting CRC metastasis, we performed gene co-expression analysis by using TCGA database data. The results demonstrated a slight positive correlation between *GFRA1* mRNA expression and EMT-activating transcription factors (ZEB1, ZEB2, SNAI2, and TCF4), EMT-markers (VIM, N-cad), invasion-related factors (MMP2 and MMP9), and growth factors (TGFB2, IGF1, FGF2, and VEGFC) (Fig 5A, S5A Fig). However, there was no significant correlation between SNAI1, TWIST, CDH1 (E-cad), VEGFA, MMP7, and *GFRA1* mRNA levels in patient samples from TCGA (S5A Fig). Next, we examined whether the expression of these positively related genes were regulated by *GFRA1* methylation in CRC cells. As shown in Fig 5B and 5C, the mRNA expression of ZEB1, ZEB2, TCF4, VIM, N-cad, TGFB2, MMP2, and MMP9 was significantly increased with the target-demethylation of *GFRA1* in HCT116 and SW480 cells. In contrast, the IGF1, FGF2, VEGFC, and SNAI2 mRNA levels did not change evidently (S5B and S5C Fig), indicating that the expression of these genes is not regulated by *GFRA1* expression. Moreover, we examined the protein expression levels of EMT markers in *GFRA1* targeted demethylated CRC cells. As shown in Fig 5D, the mesenchymal markers, VIM and N-cad were upregulated in CRC cells with *GFRA1* hypomethylation. Furthermore, immunofluorescence analysis also showed an increase in VIM and N-cad expression in *GFRA1* targeted

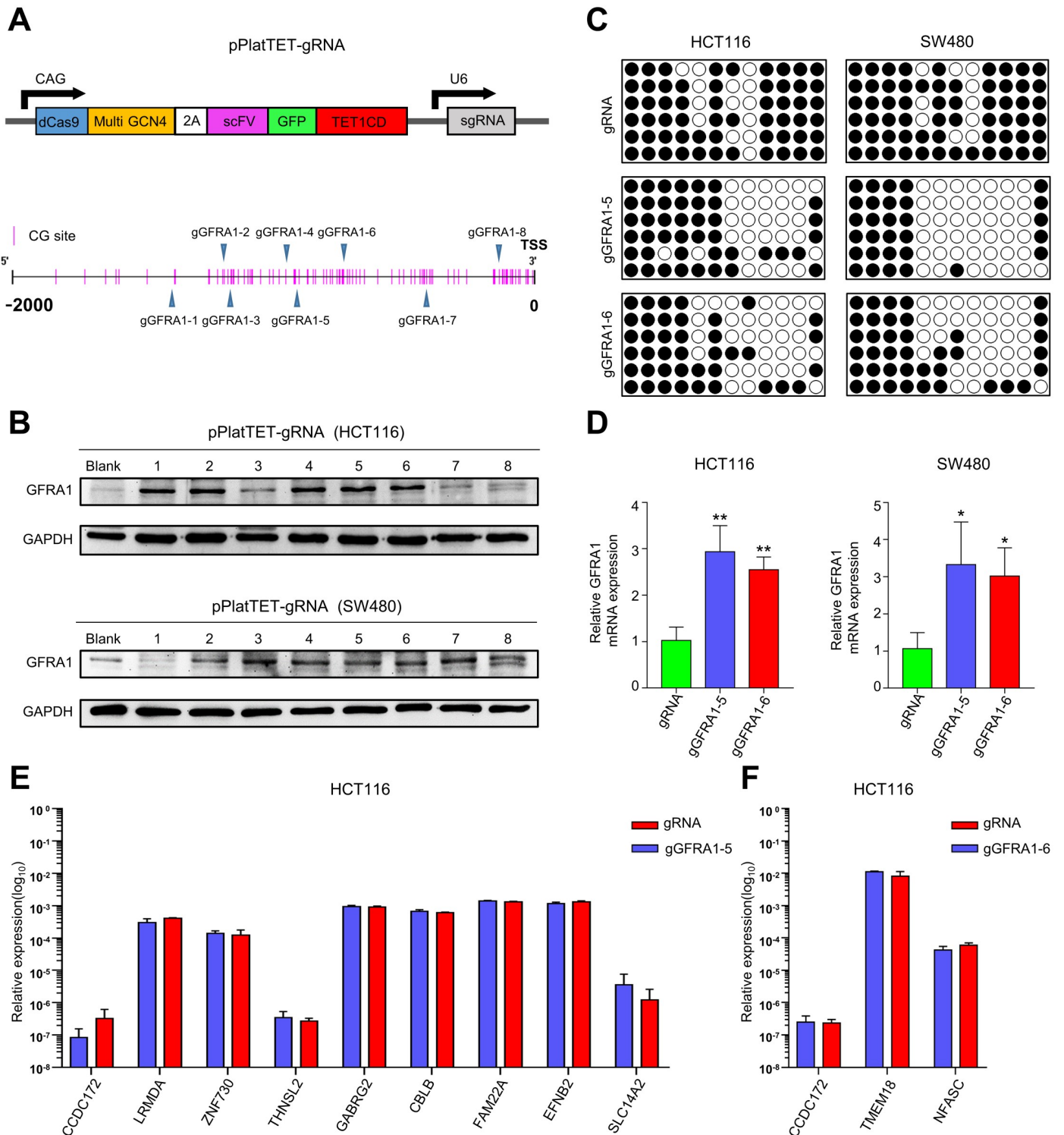


Fig 3. Targeted demethylation of *GFRA1* by dCas9-Tet1CD and verification of off-target effect in CRC cells. **A** Schematic representation of dCAS9-mediated targeted demethylation plasmid and distribution of gRNA the upstream of the *GFRA1* TSS. **B** Expression of *GFRA1* after transfection of pPlatTET-gRNA plasmids constructed from different gRNAs in HCT116 and SW480 cells was detected using western blotting. **C** BSP-seq determination of TSS region demethylation effect of pPlatTET-g*GFRA1*-5 and pPlatTET-g*GFRA1*-6 in HCT116 and SW480 cells (methylation CpG sites are shown as black dots, unmethylation CpG sites are shown as white dots). **D** The mRNA levels of *GFRA1* in *GFRA1*-targeted demethylation CRC cells detected by Real-time PCR analysis (**p* < 0.05, ***p* < 0.01; student t-test). **E-F** The relative expression of genes at g*GFRA1*-5 and g*GFRA1*-6 off-target sites in HCT116 cells (Student's t-test). Data are mean ± SD.

<https://doi.org/10.1371/journal.pgen.1009159.g003>

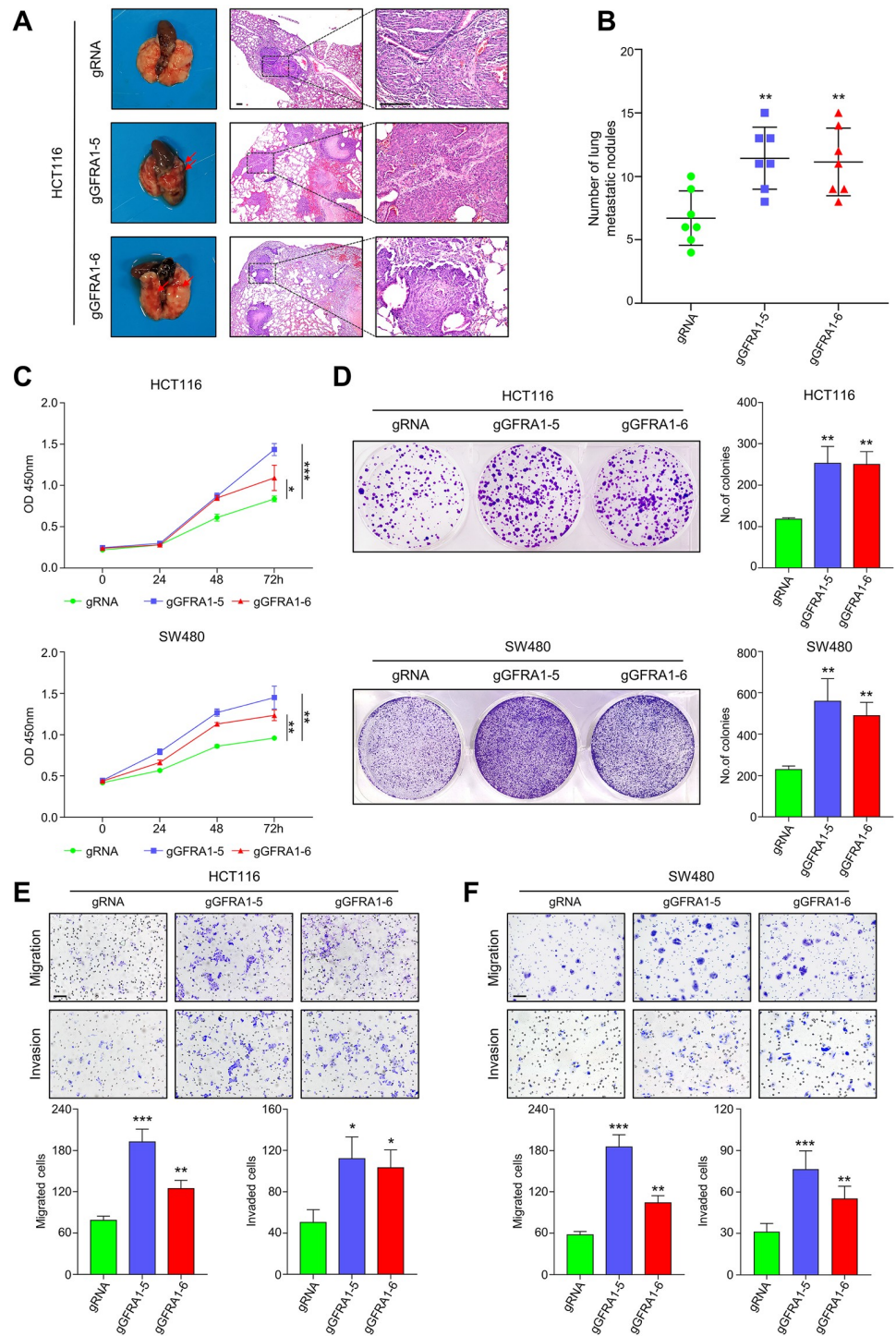


Fig 4. Hypomethylation of *GFRA1* promotes metastasis of CRC. A-B Female BALB/c nude mice were injected in tail vein with either HCT116 cells with targeted demethylation of *GFRA1* (pPlatTET-gGFRA1-5 and pPlatTET-gGFRA1-6) or respective control cells (pPlatTET-gRNA), n = 7 mice per group. Representative hematoxylin and eosin-stained images presented to show tumor lesions in the lungs (scale bar, 100 μ m). The scatter plots show the number of lesions in the lungs as mean \pm SD (**p < 0.01; Student's t-test). C CCR8 experiment demonstrates the effect of *GFRA1* demethylation on cell proliferation in HCT116 and SW480 cells (*p < 0.05, **p < 0.01, ***p < 0.001; Student's t-test). D Effects of the loss of *GFRA1* methylation on clonogenic spheroid formation in CRC cells was detected by clonogenic spheroid formation assay (**p < 0.01; student t-test). E-F Effects of *GFRA1* hypomethylation on cell migration and invasion, as evaluated by Transwell assays in CRC cells (*p < 0.05, **p < 0.01, ***p < 0.001; Student's t-test), and data are mean \pm SD from at least three independent experiments. Scale bars represent 100 μ m.

<https://doi.org/10.1371/journal.pgen.1009159.g004>

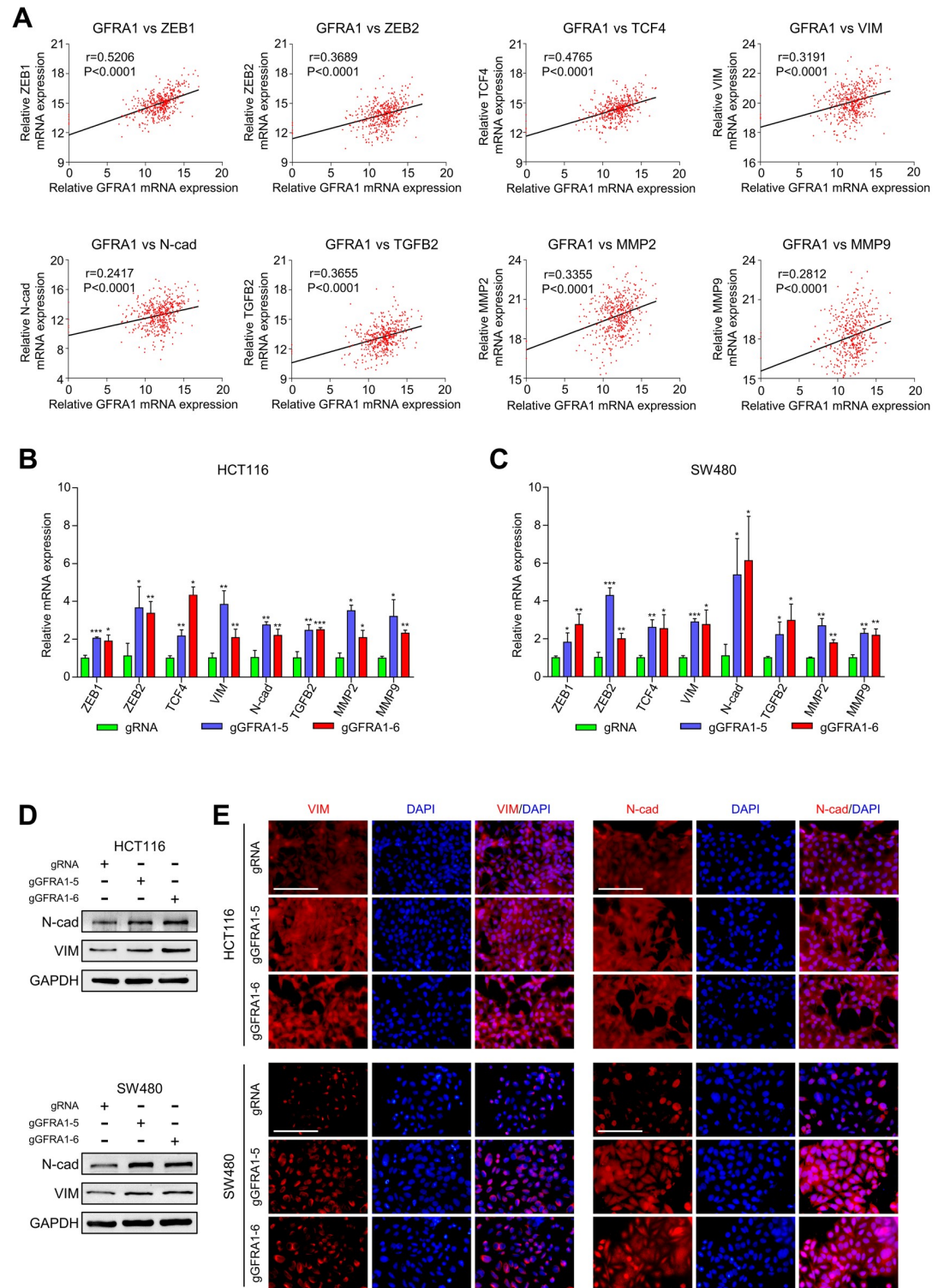


Fig 5. GFRA1 hypomethylation activates EMT in CRC cells. A Gene co-expression analysis showing the correlation of GFRA1 to ZEB1, ZEB2, TCF4, VIM, N-cad, TGFB2, MMP2, and MMP9 (Pearson correlation test). B-C q-PCR assays display the effects on gene expression (A) in GFRA1 hypomethylation CRC cells (* $p < 0.05$, ** $p < 0.01$, *** $p < 0.001$; Student's t-test). D Western blot analyses showing the effects of GFRA1-targeted demethylation on the expression of EMT marker (VIM and N-cad) proteins in CRC cells. E Immunofluorescence assays depicting localization and protein expression of EMT markers after GFRA1 demethylation. Data are mean \pm SD from at least three independent experiments. Scale bars represent 100 μ m.

<https://doi.org/10.1371/journal.pgen.1009159.g005>

demethylation HCT116 and SW480 cells, as compared to that in the control cells (Fig 5E). Taken together, our data indicated that *GFRA1* hypomethylation promoted metastasis through the induction of the EMT program in CRC cells.

Hypomethylation of *GFRA1* induces epithelial to mesenchymal transition by promoting AKT phosphorylation and upregulating c-Jun expression in CRC

To elucidate the mechanism of EMT induced by *GFRA1* hypomethylation in CRC cells, we performed *GFRA1* related pathway commons network analysis by using data from the public pathway and interactions databases (<http://www.pathwaycommons.org/>). The *GFRA1* gene was found to be associated with AKT phosphorylation and expression of Jun in CRC (Fig 6A). Then, western blotting analysis showed that the protein expression levels of p-AKT, c-Jun, and p-c-Jun were much higher in the *GFRA1*-hypomethylated cells than in their respective control cells (Fig 6B). To determine whether *GFRA1* demethylation induces EMT by promoting AKT and c-Jun phosphorylation in CRC, the AKT inhibitor MK-2206 2HCl and JNK inhibitor SP600125 were added at a concentration of 2 μ M for 48 h to the *GFRA1* targeted demethylation CRC cells. The mRNA expression levels of ZEB1, ZEB2, VIM, and N-cad were decreased after treatment of *GFRA1*-hypomethylation cells with MK-2206 2HCl and SP600125 at 2 μ M for 24 h (Fig 6C and 6D). Moreover, the protein expression levels of VIM and N-cad were lower with the reduction of p-AKT and p-c-Jun proteins in *GFRA1*-target demethylation HCT116 and SW480 cells, which was consistent with the mRNA expression data (Fig 6E and 6F). In addition, the proliferation and migration of SW480-*GFRA1* and HCT116-*GFRA1* hypomethylated cells were reduced by treatment with the inhibitors, MK-2206 2HCl and SP600125 (Fig 6G and 6H), suggesting that the promotion of *GFRA1* hypomethylation in the CRC cell proliferation and invasion can be blocked by p-AKT and p-c-Jun inhibitors. All of these results demonstrate that hypomethylation of *GFRA1* promotes AKT phosphorylation and upregulates c-Jun expression, thereby, activating EMT to promote tumor invasion in CRC.

Discussion

Tumor metastasis is the main cause of poor prognosis of CRC, thus, early predictive diagnosis of highly metastatic CRC will be helpful for the clinical treatment of patients [30, 31]. In our study, we have demonstrated that *GFRA1* hypomethylation accompanied with upregulation of *GFRA1* in invasive CRC, and correlated with poor prognosis of patients. The targeted demethylation of *GFRA1* by dCas9-TET1CD and specific gRNA promoted proliferation, migration, and metastasis of CRC cells *in vitro* and *in vivo*. Demethylation of *GFRA1* induced EMT in CRC by promoting AKT phosphorylation and increasing the AKT expression in CRC cells. Collectively, our findings indicate that *GFRA1* demethylation promotes CRC invasion *via* inducing EMT, and *GFRA1* methylation can be used a biomarker for early diagnosis of highly metastatic CRC.

DNA methylation, one of the most important factors driving tumorigenesis, are recognized as diagnosis biomarker of various cancers [6, 32, 33]. Previous studies have demonstrated the *GFRA1* methylation level was significantly decreased in gastric carcinoma with lymph/distant metastasis. Compared with patients with *GFRA1* high methylation, those with *GFRA1* low methylation had a poor relapse-free survival [5, 34]. These results indicated that *GFRA1* promotes the metastasis in gastric carcinoma. In contrast, in hepatocellular carcinoma, the higher expression of *GFRA1* was significantly correlated with good prognosis of patients [35]. In the present study, we revealed that *GFRA1* has lower methylation modification and higher

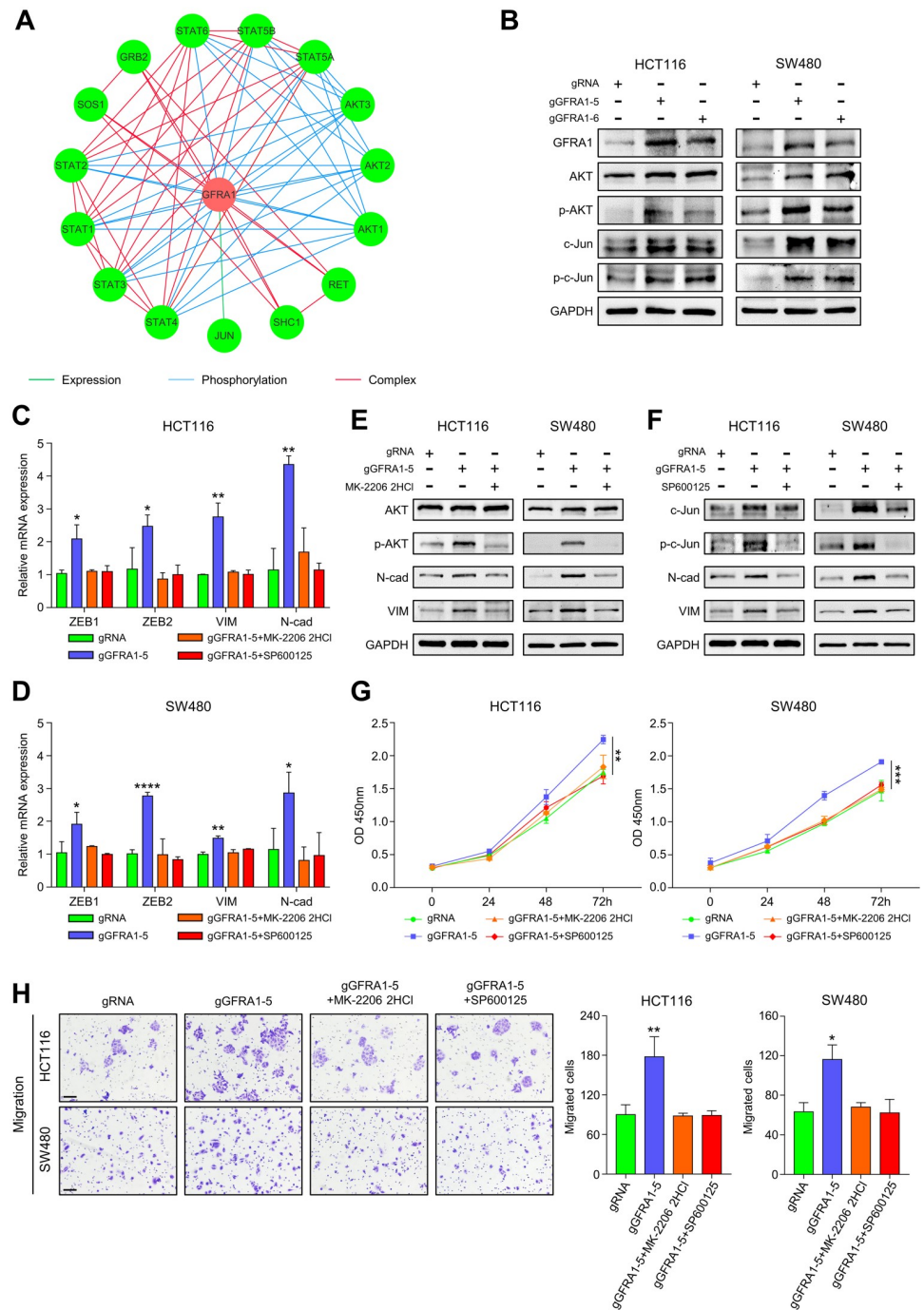


Fig 6. Hypomethylation of *GFRA1* leads to EMT being blocked by p-AKT and p-C-Jun inhibitors. **A** Pathway Common network conducted by *GFRA1* related genes. The nodes represent genes, edges display an interaction between query genes (Green line: control expression; Blue line: control Phosphorylation; Red line: in complex). **B** Western blot analyses display the effects of *GFRA1* hypomethylation on the protein expression of AKT, p-AKT, c-Jun, and p-c-Jun in HCT116 and SW480 cells. **C-D** The mRNA expression levels of ZEB1, ZEB2, VIM, and N-cad in *GFRA1* hypomethylation CRC cells treated with MK-2206 2HCl and SP600125 or DMSO, were detected by q-PCR (* $p < 0.05$, ** $p < 0.01$, **** $p < 0.0001$; Student's t-test). **E-F** Western blot analyses showing the protein expression of AKT, p-AKT, c-Jun, and p-c-Jun in HCT116-g*GFRA1*-5 and SW480-g*GFRA1*-5 cells treated with MK-2206 2HCl (E) and SP600125(F) or DMSO. **G** CCK8 experiment demonstrates the effect of treatment with MK-2206 2HCl and SP600125 on cell proliferation in *GFRA1* targeted demethylation cells (** $p < 0.01$, *** $p < 0.001$; Student's t-test). **H** Effects of MK-2206 2HCl and SP600125 treatment on cell migration in *GFRA1* hypomethylation CRC cells, as evaluated by Transwell assays. (* $p < 0.05$, ** $p < 0.01$; Student's t-test), and the data are mean \pm SD from at least three independent experiments. Scale bars represent 100 μ m.

<https://doi.org/10.1371/journal.pgen.1009159.g006>

expression in CRC invasive tumors as compared to non-invasive tumors. It also had been found that GFRA1 mRNA expression can be modulated by *GFRA1* methylation. Moreover, we noted CRC patients with GFRA1 high expression had poor overall survival and disease-free survival. Collectively, our results indicating that *GFRA1* methylation may have diagnostic potential for high metastatic CRC.

The accurate detection of DNA methylation location is essential for the understanding of regulating function of DNA methylation on the gene expression and cancer biological behaviors. [36–38]. The *GFRA1* methylation was significantly lower in CRC primary tumors with invasion, indicated that GFRA1 gene regions has the potential as a methylation biomarker for diagnosis and prediction of highly metastatic CRC. However, identification of a sequence that would be suitable as a methylation biomarker in GFRA1 gene remains unclear. For this reason, we further perform a functional analysis of the GFRA1 gene all-long using 450k methylation array data from TCGA. Results show that ten sequences in GFRA1 gene TSS region has lower methylation modifications in tumors with invasion compared to tumors without invasion. Among them, compared to tumors without invasion, the methylation level of the sequences downstream TSS is more obvious than of the sequences upstream of TSS in tumors with invasion. This phenomenon may be caused by different function of methylation modification [39]. Besides, ROC curve analysis suggests that these sequences have diagnostic value for CRC metastasis risk assessment and prediction; it is pretty helpful for metastatic CRC risk-tailored early diagnostic and primary treatment strategies. These sequences can also be combined with multiple indicators to improve the accuracy of diagnosis in clinical applications.

In terms of functionality, GFRA1 gene is involved in neurodevelopment [20, 21, 40] and spermatogenic stem cells differentiation [23, 41]. Meanwhile, ablation of GFRA1 may cause a Hirschsprung's disease phenotype [42, 43]. In cancer promotion function, GFRA1 gene can encode GFRA1 protein to promote tumor progression by activating RET and downstream pathways in breast cancer and pancreatic cancer [26, 27, 44]. Furthermore, GFRA1 gene can also guide the generation of circRNA to regulate microRNA as an oncogene in breast cancer and ovarian cancer [45, 46]. These results explain that GFRA1 can perform multiple functions in a tumor. According to the hypermethylation of *GFRA1* in CRC, we chose to endogenously upregulate gene expression by targeted demethylation of *GFRA1*, instead of introducing an overexpression plasmid, which would better represent the function of targeted genes in cells [29, 47, 48]. Owing to the undesirable effects caused by the global demethylation process, DAC and AZA faced the serious challenges in experimental applications [49, 50]. In our study, *GFRA1* methylation editing capability to efficiently address the causal-effect relationships of *GFRA1* methylcytosine epigenetic in CRC invasion. Moreover, these results for off-target predictions also confirmed the specificity of dcas9-TET1CD-gGFRA1-5 and dcas9-TET1CD-gGFRA1-6 on demethylation of the GFRA1 promoter. *In vitro* experiments indicated that the migration and invasion of CRC cells were promoted by targeted demethylation of *GFRA1*. Meanwhile, more lung metastasis nodes were observed in the groups with *GFRA1* hypomethylation. However, we failed performing GFRA1 knockdown experiments due to no CRC cell line was identified with high endogenous GFRA1 expression. Importantly, our results indicated that *GFRA1* demethylation induced EMT in CRC cells and GFRA1 mRNA expression are highly correlated with expression of EMT-related factors in CRC tissues. These results suggested that GFRA1 promote invasion and metastasis through inducing EMT in CRC cells, which would expand the understanding of GFRA1 function.

Based on the inducing role of GFRA1 on EMT, Pathway Commons analysis was employed to determine the potential downstream targets of GFRA1. We found that GFRA1 is associated with AKT phosphorylation and c-Jun expression, which induce EMT in several cancers [51, 52]. Further results suggested that *GFRA1* demethylation promotes AKT phosphorylation and

upregulates p-c-Jun and c-Jun expression. Furthermore, treatment of CRC cells with specific inhibitors targeting AKT or JNK could efficiently attenuate EMT mediated by demethylation of *GFRA1* in CRC cells. These findings suggested that GFRA1 induces EMT via AKT and c-Jun pathway. Meanwhile, AKT and JNK inhibitors would be an efficient therapy strategy for the CRC patients with *GFRA1* hypomethylation.

In summary, our findings indicate that GFRA1 functions as a tumor promoting factor to promote CRC invasion through inducing EMT. Methylation of *GFRA1* in CRC tissues can be a biomarker for diagnosis of highly metastatic CRC.

Materials and methods

Ethics statement

The CRC patient samples were obtained from the West China Hospital (Chengdu, P.R. China) with written informed consent, and the study was approved by West China Hospital of Sichuan University Biomedical Research Ethics Committee (S1 Text, Number: 2018(280)). Data including clinical information was acquired from the medical records. All mouse experimental procedures were approved by the Institutional Animal Care and Use Committees of Stake Key Laboratory of Biotherapy, Sichuan University (S2 Text, Number: 20181107004).

Bioinformatic analysis

Expression profiles of mRNA, Illumina Human Methylation 450 K array data (β -value), and clinical information of CRC patients were downloaded from The Cancer Genome Atlas (TCGA v19.0; <http://cancergenome.nih.gov/>) database. β -value was used to measure the percentage of methylation [53–55]. β -value is defined as:

$$\beta = \frac{\max(\text{methylated}, 0)}{\max(\text{methylated}, 0) + \max(\text{unmethylated}, 0) + \alpha}$$

Methylated and unmethylated are the intensity value from methylated and unmethylated probes and α is a constant offset (by default, $\alpha = 100$). β -values range from 0 (completely unmethylated) to 1 (completely methylated).

The TCGA-CRC dataset contained a total of 521 CRC samples included 41 cases of paracancerous tissues and 480 cases of tumor tissues. The age of the samples is from 31 to 90 with the median age of 68. Numbers of female and male patients is 225 and 255, respectively. Differential expression and methylation level analysis was performed on the TCGA-CRC dataset using Limma package in R (version 3.5.1) software (<https://www.r-project.org/>). Wilcoxon rank-sum test was used to compare the difference of the expression of RNA-seq and methylation data between tumor tissues and adjacent tissue. A false discovery rate (FDR) < 0.05 and $|\log_2 \text{fold change (FC)}| > 1$ was set as the criteria for screening differentially expressed and methylation genes. Comparisons between tumor invasion (lymphatic and venous invasion) and no invasion were tested by two-tailed Student's t-test, $p < 0.05$ was considered statistically significant.

GFRA1 gene CpG sites methylation level in CRC cell lines were downloaded from Cancer Cell Line Encyclopedia (CCLE 2019; <https://portals.broadinstitute.org/ccle>). GFRA1 related pathway commons network data were downloaded from the Public Pathway and Interactions Database [56] (2019 update; <http://www.pathwaycommons.org/>). Cytoscape software (version 3.7.0) was used to analyze functional pathways.

DNA methylation analyses

The DNA extraction was performed using Tissue & Cell Genomic DNA Purification Kit (GeneMark #DP201). DNA and methylation quality analyses identified 75 CRC samples and 17 paracancerous samples suitable for the methylation study. To verify the results of methylation analysis of GFRA1 gene based on TCGA data, sequence (including parts of cg25617725 and cg12087643 sequence) upstream of the GFRA1 gene TSS was selected for time-of-flight mass spectrometry to determine methylation modification levels.

Cell culture and plasmid transfection

Human colorectal cancer cells, HCT116, SW480, HT29, and RKO were maintained in Dulbecco's modified Eagle's medium (Gibco) supplemented with 10% fetal bovine serum (Gibco, MA, USA). All cell lines were maintained at 37°C with 5% CO₂. The empty plasmid pPlat-TET1-gRNA (Addgene plasmid: 82559) and GFRA1-targeted demethylation plasmid from pPlatTET1-gRNA1 to pPlatTET1-gRNA8 (the sequences of gRNA are displayed in Table S3) were transfected into HCT116 and SW480 cells using Lipofectamine 3000 reagent (Invitrogen #2024201, MA, USA), according to the manufacturer's instructions. Successful transfection was verified as green fluorescence under fluorescence microscope. G418 (Sigma-aldrich #A1720, MA, USA) with a concentration of 2 g/L for 48 h was added for screening. After that, the HCT116 and SW480 cells transfected with the plasmid were used in subsequent experiments.

Murine experimental lung metastasis experiments

Female BALB/c nude mice at 6 weeks of age were purchased from HFK Bioscience (Beijing, P. R. China). All mice were bred in the Animal Experimentation Unit (Sichuan University, Chengdu, China). Twenty one mice were randomly divided into three groups. Then, HCT116-pPlatTET-gRNA cells (control cells), HCT116-pPlatTET-gGFRA1-5 cells, and HCT116-pPlatTET-gGFRA1-6 cells (5×10^5 cells/ mouse) were injected into the tail vein of each mouse. Mice were anaesthetised by intraperitoneal injection of 1% sodium pentobarbital (100 µl/ mouse). All mice were sacrificed after one month and the lung tissues were removed for histological examination. After that, the mice lungs were fixed in 4% PFA for 48 h and embedded in paraffin, 5 µm sections were cut, and stained with hematoxylin and eosin (H&E).

Reverse transcription and quantitative PCR (qRT-PCR)

CRC cells and CRC patient samples were harvested using Trizol (Ambin #15596026, CA, USA), according to manufacturer's instructions. RNA was converted to cDNA using Prime-Script RT reagent Kit with gDNA Eraser (Perfect Real Time) (Takara #RR047B, Tokoyo, Japan). Quantitative PCR reactions were prepared with TB green Premix EX TaqII (Takara #RR820A, Tokoyo, Japan), and performed in Light Cycler 96 System (Roche, Switzerland). Primer sequence information for RT-qPCR is listed in [S5 Table](#).

Western blotting

CRC cells and patient samples were lysed using RIPA lysis buffer containing proteinase inhibitor (1:100, Invitrogen #87785), and was subjected to immunoblot analysis. Mouse anti-GFRA1 (1:1000, Santacruz #sc-271546, MA, USA), rabbit anti-VIM (1:1000, Cell Signaling #5741, CA, USA), rabbit anti-N-cad (CDH2) (1:1000, ServiceBio #GB11135, Wuhan, China), rabbit anti-AKT (1:1000, Cell Signaling #4691, CA, USA), rabbit anti-p-AKT (1:1000, Cell Signaling #4060, CA, USA), rabbit anti C-Jun (1:1000, Cell Signaling #6195, CA, USA), and rabbit anti

p-C-Jun (1:1000, Cell Signaling #3270, CA, USA) antibodies were used. Decitabine (DAC), MK-2206 2HCl and SP600125 was purchased from Selleck.

Immunohistochemistry and immunofluorescence

For immunohistochemistry (IHC), patient tissues were fixed in 4% Paraformaldehyde, embedded in paraffin, and then cut into 5 μ m thick sections for IHC staining. The slides were blocked with non-immune goat serum and incubated with anti-mouse GFRA1 antibody (1:200 Santa-cruz #sc-271546) for 24 h at 4°C. Then follow the instructions (ZSGB-BIO #SP-9002, Beijing, China).

For immunofluorescence, the transfected HCT116 cells and SW480 cells grown on the cover glass in 24 well plates were fixed with 4% paraformaldehyde (PFA) for 20 min and permeabilized with 0.2% Triton X-100 for 15 min at room temperature (22–25°C). Then, the cells were incubated with the desired primary antibodies in PBS for 24 h at 4°C, washed with PBS 3 times, and then incubated with fluorescent secondary antibodies away from light at room temperature (22–25°C). After that, the nuclei were stained with DAPI. The fluorescence intensity and absorbance were measured at 555 nm (Invitrogen #A21428, MA, USA) and 488 nm (Invitrogen #A11001, MA, USA), respectively.

Bisulfite sequencing PCR

Bisulfite Sequencing (BSP-seq) of all bisulfite converted genomic DNA samples was performed with DNA Bisulfite Conversion Kit (TIANGEN # DP215-02), according to the manufacturer's instructions. The primer sequences that were used are as follows:

GFRA1-F1 5'-GTTTTAGGAGAGAGGTAGAGATTG-3'

GFRA1-R1 5'-AATACTACCAAACACACACTCT-3'

GFRA1-F2 5'-GCGTATTTTAGGATCGTTCG-3'

GFRA1-R2 5'-CAAAACACGCAATATTCTACA-3'

PCR reactions were done using EpiTaq HS (TaKaRa #R110Q, Tokoyo, Japan). After purifying the PCR product by GEL Extraction Kit (OMEGA # D2500-01), this DNA fragment was subsequently cloned into pClone007 Simple Vector (TSINGKE #TSV-007S, Beijing, China) for sequencing. Methylation levels of CpG site in GFRA1 gene fragments were analyzed by QUMA (<http://quma.cdb.riken.jp/>).

Cell proliferation and clonogenic assay

For CCK8 cell proliferation assay, HCT116 (5000 cells/ per well) and SW480 (10000 cells/ per well) cells were plated in four 96 well plates with three repeated wells assigned for each group. Absorption values were measured 2 h after adding CCK8 reagent (DOJINDO #CK04), every 24 h. The optical density (OD) was measured at 450 nm.

For cell clonogenic assay, the transfected HCT116 cells (1000 cells/ well) and SW480 cells (5000 cells/ well) were replated in the 6 well plates, and cultured in complete medium for 2 weeks. Then, the cells were stained with crystal violet and the individual colonies were counted.

Migration and invasion assays

Cell culture insert transparent PET Membrane, 24 Well, 8.0 μ m pore size (Falcon #353097) were used for the migration and invasion assays. A total of 600 μ l of culture medium containing 20% FBS (Gibco, MA, USA) was added to the lower chamber. In the migration assay, 1×10^5 GFRA1-hypomethylation HCT116 or SW480 cells and their respective control cells in

100 μ l serum-free medium were plated on the uncoated insets, and were incubated for 48 h. In the invasion assay, the insets were coated with 60 μ l of 1:10-diluted matrigel (BD Biosciences, MA, USA), and 1.5×10^5 cells in 100 μ l serum-free medium were plated on the insets for an incubation period of 48 h. After that, the cells attached to the membrane were fixed with 4% PFA for 20 min, stained with 5% crystal violet (Beyotime #C0121, Beijing, China) 10 min, and counted at 100x magnification.

Statistical analysis

Statistical analysis was performed using GraphPad software (version 8.00) and $p < 0.05$ was considered statistically significant. Comparisons between the two groups were analyzed by two-tailed Student's t-test. Receiver operating characteristic (ROC) curve analysis was used to test the effectiveness of the methylation level of the GFRA1 DNA probe for the diagnosis of invasive CRC tumors. Correlation analysis was evaluated by Pearson's correlation test. Survival was determined by log-rank (Mantel-Cox) test. Measurement data are mean \pm SD from at least three independent experiments.

Supporting information

S1 Fig. Methylation of *GFRA1* can regulate gene expression. **A** Venn diagram showing the number of genes with methylation modification and significantly reduced expression levels from TCGA CRC RNA-seq data and methylation data (FDR < 0.05 , Wilcoxon rank-sum test). **B** Heat map showing associated with the expression profile of 65 genes in normal and tumor tissues from S1A Fig, gene expression levels are represented by the color of the heat map (red means high expression, green means low expression). **C** Q-PCR analysis showing the expression level of GFRA1 in HCT116 and SW480 cells after treatment gradient concentration DAC for 48h. (** $p < 0.01$, *** $p < 0.01$, **** $p < 0.0001$ student t-test). **D** Western blot analyses display the effects of DAC on the protein expression of GFRA1 in HCT116, SW480, HT29 and RKO. **E** Immunofluorescence assays display localization and expression of GFRA1 in HCT116 and SW480 cells treated with DAC. Scale bars, 100 μ m. **F** Immunohistochemical analysis of GFRA1 expression in primary tumor tissue from HXCRC cohort TMA. Scale bars, 100 μ m. (TIF)

S2 Fig. Methylation levels are significantly associated with gene expression and tumor invasion in the downstream sequences of *GFRA1* TSS. **A-G** Detailed description of seven methylation sequences upstream of GFRA1 gene TSS from (Fig 2C), including correlation between gene expression and DNA methylation, Variety in DNA methylation levels at different tumor stages and Differences in methylation levels between invasive and non-invasive tumors (* $p < 0.05$, ** $p < 0.01$, *** $p < 0.01$, **** $p < 0.0001$ student t-test). (TIF)

S3 Fig. ROC curves for the diagnosis of CRC Lymphatic invasion by *GFRA1* TSS sequences. **A** ROC curves for cg13320291. **B** ROC curves for cg24792682. **C** ROC curves for cg06298519. **D** ROC curves for cg19485539. **E** ROC curves for cg17256532. **F** ROC curves for cg19236679. **G** ROC curves for cg03503087. **H** ROC curves for cg25617725. (TIF)

S4 Fig. *GFRA1* TSS CpG methylation level in CRC cell lines. **A** Heatmap visualization of GFRA1 gene CpG sites methylation level in CRC cells form CCLE database. (Those sites with no data in CRC cell lines were colored in grey). **B** BSP-seq showing the methylation level in HCT116 and SW480 cells (methylation CpG sites are shown as black dots, unmethylation CpG sites are shown as white dots). **C-D** The relative expression of genes at gGFRA1-5 and

gGFRA1-6 off-target sites in SW480 cells (Student's t-test). Data are mean \pm SD.
(TIF)

S5 Fig. Genes that do not show a correlation at the expression level with targeted removal of GFRA1 methylation in CRC cells. A Gene co-expression analysis display the correlation between of GFRA1 and IGF1, FGF2, VEGFC, VEGFA, MMP7, CDH1, TWIST1, SNAI1, SNAI2 (Pearson correlation test). B-C Q-PCR showing the effects of IGF1, FGF2, VEGFC, SNAI2 expression in GFRA1 demethylation HCT116 and SW480 cells (student t-test).
(TIF)

S1 Table. 450k probe sequences related to CRC invasion.
(DOCX)

S2 Table. gRNA sequences about GFRA1 gene targeted demethylation.
(DOCX)

S3 Table. gRNA5 sequence predicted off-target sites.
(DOCX)

S4 Table. gRNA6 sequence predicted off-target sites.
(DOCX)

S5 Table. q-PCR primer sequences.
(DOCX)

S1 Text. Human ethics certification.
(PDF)

S2 Text. Animal experiment ethics certification.
(PDF)

Acknowledgments

Thanks to Chengdu Basebiotech Co., Ltd for providing assistance on bioinformatic analysis.

Author Contributions

Conceptualization: Zhexu Dong, Lei Dai, Hongxin Deng.

Data curation: Zhexu Dong, Lei Dai, Yong Zhang, Gang Shi, Hongxin Deng.

Formal analysis: Zhexu Dong, Lei Dai, Yong Zhang.

Funding acquisition: Lei Dai, Hongxin Deng.

Investigation: Zhexu Dong, Lei Dai, Yong Zhang.

Methodology: Zhexu Dong, Gang Shi, Qin Wang, Yi Liu, Yi Lin, Yuan Wang, Qingnan Wang, Huiling Wang, Hantao Zhang, Yujing Zhang, Xiaolan Su, Hongxin Deng.

Project administration: Zhexu Dong.

Resources: Lei Dai, Yong Zhang, Chao Fang, Ye Chen, Feng Wang, Meng Qiu, Zongguang Zhou.

Software: Zhexu Dong, Yong Zhang.

Supervision: Gang Shi, Lin Cheng, Shuang Zhang.

Validation: Zhexu Dong, Junshu Li, Jiamei Fu, Yan Yu, Wenshuang Wang.

Visualization: Zhexu Dong, Yong Zhang.

Writing – original draft: Zhexu Dong.

Writing – review & editing: Zhexu Dong, Lei Dai, Yong Zhang, Gang Shi, Hongxin Deng.

References

1. Bray F, Ferlay J, Soerjomataram I, Siegel RL, Torre LA, Jemal A. Global cancer statistics 2018: GLOBOCAN estimates of incidence and mortality worldwide for 36 cancers in 185 countries. *CA Cancer J Clin*. 2018; 68(6):394–424. Epub 2018/09/13. <https://doi.org/10.3322/caac.21492> PMID: 30207593.
2. Van Cutsem E, Cervantes A, Nordlinger B, Arnold D, Group EGW. Metastatic colorectal cancer: ESMO Clinical Practice Guidelines for diagnosis, treatment and follow-up. *Ann Oncol*. 2014; 25 Suppl 3:iii1–9. Epub 2014/09/06. <https://doi.org/10.1093/annonc/mdu260> PMID: 25190710.
3. Chen J, Sun H, Tang W, Zhou L, Xie X, Qu Z, et al. DNA methylation biomarkers in stool for early screening of colorectal cancer. *J Cancer*. 2019; 10(21):5264–71. Epub 2019/10/12. <https://doi.org/10.7150/jca.34944> PMID: 31602277
4. Li WH, Zhang H, Guo Q, Wu XD, Xu ZS, Dang CX, et al. Detection of SNCA and FBN1 methylation in the stool as a biomarker for colorectal cancer. *Dis Markers*. 2015; 2015:657570. Epub 2015/03/25. <https://doi.org/10.1155/2015/657570> PMID: 25802477
5. Liu Z, Cheng X, Zhang L, Zhou J, Deng D, Ji J. A panel of DNA methylated markers predicts metastasis of pN0M0 gastric carcinoma: a prospective cohort study. *Br J Cancer*. 2019; 121(7):529–36. Epub 2019/08/23. <https://doi.org/10.1038/s41416-019-0552-0> PMID: 31431673
6. Carethers JM, Jung BH. Genetics and Genetic Biomarkers in Sporadic Colorectal Cancer. *Gastroenterology*. 2015; 149(5):1177–90 e3. Epub 2015/07/29. <https://doi.org/10.1053/j.gastro.2015.06.047> PMID: 26216840
7. Stuelten CH, Parent CA, Montell DJ. Cell motility in cancer invasion and metastasis: insights from simple model organisms. *Nat Rev Cancer*. 2018; 18(5):296–312. Epub 2018/03/17. <https://doi.org/10.1038/nrc.2018.15> PMID: 29546880
8. Hanahan D, Weinberg RA. Hallmarks of cancer: the next generation. *Cell*. 2011; 144(5):646–74. Epub 2011/03/08. <https://doi.org/10.1016/j.cell.2011.02.013> PMID: 21376230.
9. Das V, Kalita J, Pal M. Predictive and prognostic biomarkers in colorectal cancer: A systematic review of recent advances and challenges. *Biomed Pharmacother*. 2017; 87:8–19. Epub 2017/01/04. <https://doi.org/10.1016/j.biopha.2016.12.064> PMID: 28040600.
10. Puccini A, Lenz HJ. Colorectal cancer in 2017: Practice-changing updates in the adjuvant and metastatic setting. *Nat Rev Clin Oncol*. 2018; 15(2):77–8. Epub 2017/11/29. <https://doi.org/10.1038/nrclinonc.2017.185> PMID: 29182161.
11. Widschwendter M, Jones A, Evans I, Reisel D, Dillner J, Sundstrom K, et al. Epigenome-based cancer risk prediction: rationale, opportunities and challenges. *Nat Rev Clin Oncol*. 2018; 15(5):292–309. Epub 2018/02/28. <https://doi.org/10.1038/nrclinonc.2018.30> PMID: 29485132.
12. Belinsky SA. Gene-promoter hypermethylation as a biomarker in lung cancer. *Nat Rev Cancer*. 2004; 4(9):707–17. Epub 2004/09/03. <https://doi.org/10.1038/nrc1432> PMID: 15343277.
13. Andresen K, Boberg KM, Vedeld HM, Honne H, Jebsen P, Hektoen M, et al. Four DNA methylation biomarkers in biliary brush samples accurately identify the presence of cholangiocarcinoma. *Hepatology*. 2015; 61(5):1651–9. Epub 2015/02/04. <https://doi.org/10.1002/hep.27707> PMID: 25644509
14. Rasmussen SL, Krarup HB, Sunesen KG, Pedersen IS, Madsen PH, Thorlacius-Ussing O. Hyper-methylated DNA as a biomarker for colorectal cancer: a systematic review. *Colorectal Dis*. 2016; 18(6):549–61. Epub 2016/03/22. <https://doi.org/10.1111/codi.13336> PMID: 26998585.
15. Murakami T, Kikuchi H, Ishimatsu H, Iino I, Hirotsu A, Matsumoto T, et al. Tenascin C in colorectal cancer stroma is a predictive marker for liver metastasis and is a potent target of miR-198 as identified by microRNA analysis. *Br J Cancer*. 2017; 117(9):1360–70. Epub 2017/10/25. <https://doi.org/10.1038/bjc.2017.291> PMID: 29065427
16. Liu R, Su X, Long Y, Zhou D, Zhang X, Ye Z, et al. A systematic review and quantitative assessment of methylation biomarkers in fecal DNA and colorectal cancer and its precursor, colorectal adenoma. *Mutat Res*. 2019; 779:45–57. Epub 2019/05/18. <https://doi.org/10.1016/j.mrrev.2019.01.003> PMID: 31097151.
17. Sina AA, Carrascosa LG, Trau M. DNA Methylation-Based Point-of-Care Cancer Detection: Challenges and Possibilities. *Trends Mol Med*. 2019; 25(11):955–66. Epub 2019/06/30. <https://doi.org/10.1016/j.molmed.2019.05.014> PMID: 31253589.

18. Hashimoto Y, Zumwalt TJ, Goel AJE. DNA methylation patterns as noninvasive biomarkers and targets of epigenetic therapies in colorectal cancer. *Epigenomics*. 2016;epi-2015-0013. <https://doi.org/10.2217/epi-2015-0013> PMID: 27102979
19. Kim M, Kim DJ. GFRA1: A Novel Molecular Target for the Prevention of Osteosarcoma Chemoresistance. *Int J Mol Sci*. 2018; 19(4). Epub 2018/04/05. <https://doi.org/10.3390/ijms19041078> PMID: 29617307
20. Ledda F, Paratcha G, Sandoval-Guzman T, Ibanez CF. GDNF and GFRalpha1 promote formation of neuronal synapses by ligand-induced cell adhesion. *Nat Neurosci*. 2007; 10(3):293–300. Epub 2007/02/21. <https://doi.org/10.1038/nn1855> PMID: 17310246.
21. Pozas E, Ibanez CF. GDNF and GFRalpha1 promote differentiation and tangential migration of cortical GABAergic neurons. *Neuron*. 2005; 45(5):701–13. Epub 2005/03/08. <https://doi.org/10.1016/j.neuron.2005.01.043> PMID: 15748846.
22. Nakagawa T, Sharma M, Nabeshima Y, Braun RE, Yoshida S. Functional hierarchy and reversibility within the murine spermatogenic stem cell compartment. *Science*. 2010; 328(5974):62–7. Epub 2010/03/20. <https://doi.org/10.1126/science.1182868> PMID: 20299552
23. Hara K, Nakagawa T, Enomoto H, Suzuki M, Yamamoto M, Simons BD, et al. Mouse spermatogenic stem cells continually interconvert between equipotent singly isolated and syncytial states. *Cell Stem Cell*. 2014; 14(5):658–72. Epub 2014/05/06. <https://doi.org/10.1016/j.stem.2014.01.019> PMID: 24792118
24. He Z, Jiang J, Hofmann MC, Dym M. Gfra1 silencing in mouse spermatogonial stem cells results in their differentiation via the inactivation of RET tyrosine kinase. *Biol Reprod*. 2007; 77(4):723–33. Epub 2007/07/13. <https://doi.org/10.1095/biolreprod.107.062513> PMID: 17625109
25. Hammoud SS, Low DH, Yi C, Lee CL, Oatley JM, Payne CJ, et al. Transcription and imprinting dynamics in developing postnatal male germline stem cells. *Genes Dev*. 2015; 29(21):2312–24. Epub 2015/11/08. <https://doi.org/10.1101/gad.261925.115> PMID: 26545815
26. He S, Chen CH, Chernichenko N, He S, Bakst RL, Barajas F, et al. GFRalpha1 released by nerves enhances cancer cell perineural invasion through GDNF-RET signaling. *Proc Natl Acad Sci U S A*. 2014; 111(19):E2008–17. Epub 2014/04/30. <https://doi.org/10.1073/pnas.1402944111> PMID: 24778213
27. Essegir S, Todd SK, Hunt T, Poulsom R, Plaza-Menacho I, Reis-Filho JS, et al. A role for glial cell derived neurotrophic factor induced expression by inflammatory cytokines and RET/GFR alpha 1 receptor up-regulation in breast cancer. *Cancer Res*. 2007; 67(24):11732–41. Epub 2007/12/20. <https://doi.org/10.1158/0008-5472.CAN-07-2343> PMID: 18089803.
28. Kim M, Jung JY, Choi S, Lee H, Morales LD, Koh JT, et al. GFRA1 promotes cisplatin-induced chemoresistance in osteosarcoma by inducing autophagy. *Autophagy*. 2017; 13(1):149–68. Epub 2016/10/19. <https://doi.org/10.1080/15548627.2016.1239676> PMID: 27754745
29. Morita S, Noguchi H, Horii T, Nakabayashi K, Kimura M, Okamura K, et al. Targeted DNA demethylation in vivo using dCas9-peptide repeat and scFv-TET1 catalytic domain fusions. *Nat Biotechnol*. 2016; 34(10):1060–5. Epub 2016/08/30. <https://doi.org/10.1038/nbt.3658> PMID: 27571369.
30. Zellweger M, Abdelnour-Berchtold E, Krueger T, Ris HB, Perentes JY, Gonzalez M. Surgical treatment of pulmonary metastasis in colorectal cancer patients: Current practice and results. *Crit Rev Oncol Hematol*. 2018; 127:105–16. Epub 2018/06/13. <https://doi.org/10.1016/j.critrevonc.2018.05.001> PMID: 29891107.
31. Low YS, Blocker C, McPherson JR, Tang SA, Cheng YY, Wong JYS, et al. A formalin-fixed paraffin-embedded (FFPE)-based prognostic signature to predict metastasis in clinically low risk stage I/II microsatellite stable colorectal cancer. *Cancer Lett*. 2017; 403:13–20. Epub 2017/06/19. <https://doi.org/10.1016/j.canlet.2017.05.031> PMID: 28624625.
32. Han TS, Ban HS, Hur K, Cho HS. The Epigenetic Regulation of HCC Metastasis. *Int J Mol Sci*. 2018; 19(12). Epub 2018/12/14. <https://doi.org/10.3390/ijms19123978> PMID: 30544763
33. Liu F, Ma F, Wang Y, Hao L, Zeng H, Jia C, et al. PKM2 methylation by CARM1 activates aerobic glycolysis to promote tumorigenesis. *Nat Cell Biol*. 2017; 19(11):1358–70. Epub 2017/10/24. <https://doi.org/10.1038/ncb3630> PMID: 29058718
34. Liu Z, Zhang J, Gao Y, Pei L, Zhou J, Gu L, et al. Large-scale characterization of DNA methylation changes in human gastric carcinomas with and without metastasis. *Clin Cancer Res*. 2014; 20(17):4598–612. Epub 2014/07/11. <https://doi.org/10.1158/1078-0432.CCR-13-3380> PMID: 25009298
35. Zhang R, Ye J, Huang H, Du X. Mining featured biomarkers associated with vascular invasion in HCC by bioinformatics analysis with TCGA RNA sequencing data. *Biomed Pharmacother*. 2019; 118:109274. Epub 2019/09/24. <https://doi.org/10.1016/j.biopha.2019.109274> PMID: 31545220.

36. Koch A, Jeschke J, Van Criekinge W, van Engeland M, De Meyer T. MEXPRESS update 2019. *Nucleic Acids Res.* 2019; 47(W1):W561–W5. Epub 2019/05/23. <https://doi.org/10.1093/nar/gkz445> PMID: 31114869
37. Koch A, Joosten SC, Feng Z, de Ruijter TC, Draht MX, Melotte V, et al. Analysis of DNA methylation in cancer: location revisited. *Nat Rev Clin Oncol.* 2018; 15(7):459–66. Epub 2018/04/19. <https://doi.org/10.1038/s41571-018-0004-4> PMID: 29666440.
38. van Vlodrop IJ, Niessen HE, Derks S, Baldewijns MM, van Criekinge W, Herman JG, et al. Analysis of promoter CpG island hypermethylation in cancer: location, location, location! *Clin Cancer Res.* 2011; 17(13):4225–31. Epub 2011/05/12. <https://doi.org/10.1158/1078-0432.CCR-10-3394> PMID: 21558408.
39. Shukla S, Kavak E, Gregory M, Imashimizu M, Shutinoski B, Kashlev M, et al. CTCF-promoted RNA polymerase II pausing links DNA methylation to splicing. *Nature.* 2011; 479(7371):74–9. Epub 2011/10/04. <https://doi.org/10.1038/nature10442> PMID: 21964334.
40. Shepherd IT, Pietsch J, Elworthy S, Kelsh RN, Raible DW. Roles for GFRA1 receptors in zebrafish enteric nervous system development. *Development.* 2004; 131(1):241–9. Epub 2003/12/09. <https://doi.org/10.1242/dev.00912> PMID: 14660438.
41. Ferranti F, Muciaccia B, Ricci G, Dovere L, Canipari R, Magliocca F, et al. Glial cell line-derived neurotrophic factor promotes invasive behaviour in testicular seminoma cells. *Int J Androl.* 2012; 35(5):758–68. Epub 2012/04/24. <https://doi.org/10.1111/j.1365-2605.2012.01267.x> PMID: 22519471.
42. Uesaka T, Jain S, Yonemura S, Uchiyama Y, Milbrandt J, Enomoto H. Conditional ablation of GFRA1 in postmigratory enteric neurons triggers unconventional neuronal death in the colon and causes a Hirschsprung's disease phenotype. *Development.* 2007; 134(11):2171–81. Epub 2007/05/18. <https://doi.org/10.1242/dev.001388> PMID: 17507417.
43. Borrego S, Fernández RM, Dziema H, Niess A, Lópezalonso M, Antiñolo G, et al. Investigation of germline GFRA4 mutations and evaluation of the involvement of GFRA1, GFRA2, GFRA3, and GFRA4 sequence variants in Hirschsprung disease. *Journal of medical genetics.* 2003; 40(3):e18. <https://doi.org/10.1136/jmg.40.3.e18> PMID: 12624147
44. Bhakta S, Crocker LM, Chen Y, Hazen M, Schutten MM, Li D, et al. An Anti-GDNF Family Receptor Alpha 1 (GFRA1) Antibody-Drug Conjugate for the Treatment of Hormone Receptor-Positive Breast Cancer. *Mol Cancer Ther.* 2018; 17(3):638–49. Epub 2017/12/29. <https://doi.org/10.1158/1535-7163.MCT-17-0813> PMID: 29282299.
45. Liu J, Yu F, Wang S, Zhao X, Jiang F, Xie J, et al. circGFRA1 Promotes Ovarian Cancer Progression By Sponging miR-449a. *J Cancer.* 2019; 10(17):3908–13. Epub 2019/08/17. <https://doi.org/10.7150/jca.31615> PMID: 31417634
46. He R, Liu P, Xie X, Zhou Y, Liao Q, Xiong W, et al. circGFRA1 and GFRA1 act as ceRNAs in triple negative breast cancer by regulating miR-34a. *J Exp Clin Cancer Res.* 2017; 36(1):145. Epub 2017/10/19. <https://doi.org/10.1186/s13046-017-0614-1> PMID: 29037220
47. Maeder ML, Angstman JF, Richardson ME, Linder SJ, Cascio VM, Tsai SQ, et al. Targeted DNA demethylation and activation of endogenous genes using programmable TALE-TET1 fusion proteins. *Nat Biotechnol.* 2013; 31(12):1137–42. Epub 2013/10/11. <https://doi.org/10.1038/nbt.2726> PMID: 24108092
48. Wang Q, Dai L, Wang Y, Deng J, Lin Y, Wang Q, et al. Targeted demethylation of the SARI promotor impairs colon tumour growth. *Cancer Lett.* 2019; 448:132–43. Epub 2019/02/17. <https://doi.org/10.1016/j.canlet.2019.01.040> PMID: 30771439.
49. Dawson MA. The cancer epigenome: Concepts, challenges, and therapeutic opportunities. *Science (New York, NY).* 2017; 355(6330):1147–52. Epub 2017/07/22. <https://doi.org/10.1126/science.aam7304> PMID: 28302822
50. Northcott PA, Pfister SM, Jones DT. Next-generation (epi)genetic drivers of childhood brain tumours and the outlook for targeted therapies. *The Lancet Oncology.* 2015; 16(6):e293–302. Epub 2015/06/13. [https://doi.org/10.1016/S1470-2045\(14\)71206-9](https://doi.org/10.1016/S1470-2045(14)71206-9) PMID: 26065614.
51. Dongre A, Weinberg RA. New insights into the mechanisms of epithelial-mesenchymal transition and implications for cancer. *Nat Rev Mol Cell Biol.* 2019; 20(2):69–84. Epub 2018/11/22. <https://doi.org/10.1038/s41580-018-0080-4> PMID: 30459476.
52. Xue G, Restuccia DF, Lan Q, Hynx D, Dirnhofer S, Hess D, et al. Akt/PKB-mediated phosphorylation of Twist1 promotes tumor metastasis via mediating cross-talk between PI3K/Akt and TGF-beta signaling axes. *Cancer Discov.* 2012; 2(3):248–59. Epub 2012/05/16. <https://doi.org/10.1158/2159-8290.CD-11-0270> PMID: 22585995.
53. Bibikova M, Lin Z, Zhou L, Chudin E, Garcia EW, Wu B, et al. High-throughput DNA methylation profiling using universal bead arrays. *Genome Res.* 2006; 16(3):383–93. Epub 2006/02/02. <https://doi.org/10.1101/gr.4410706> PMID: 16449502

54. Du P, Zhang X, Huang CC, Jafari N, Kibbe WA, Hou L, et al. Comparison of Beta-value and M-value methods for quantifying methylation levels by microarray analysis. *BMC Bioinformatics*. 2010; 11:587. Epub 2010/12/02. <https://doi.org/10.1186/1471-2105-11-587> PMID: 21118553
55. Weinhold L, Wahl S, Pechlivanis S, Hoffmann P, Schmid M. A statistical model for the analysis of beta values in DNA methylation studies. *BMC Bioinformatics*. 2016; 17(1):480. Epub 2016/11/24. <https://doi.org/10.1186/s12859-016-1347-4> PMID: 27875981
56. Rodchenkov I, Babur O, Luna A, Aksoy BA, Wong JV, Fong D, et al. Pathway Commons 2019 Update: integration, analysis and exploration of pathway data. *Nucleic Acids Res*. 2020; 48(D1):D489–D97. Epub 2019/10/28. <https://doi.org/10.1093/nar/gkz946> PMID: 31647099